Subscriber access provided by UNIVERSITY OF MARYLAND UNIVERSITY LIBRARIES

Article

Compositions and Formation Mechanisms of Solid-Electrolyte-Interphase (SEI) on Microporous Carbon/Sulfur Cathodes

Luning Wang, Yuxiao Lin, Samantha DeCarlo, Yi Wang, Kevin Leung, Yue Qi, Kang Xu, Chunsheng Wang, and Bryan W. Eichhorn

Chem. Mater., **Just Accepted Manuscript** • DOI: 10.1021/acs.chemmater.9b05027 • Publication Date (Web): 02 Apr 2020

Downloaded from pubs.acs.org on April 7, 2020

Just Accepted

“Just Accepted” manuscripts have been peer-reviewed and accepted for publication. They are posted online prior to technical editing, formatting for publication and author proofing. The American Chemical Society provides “Just Accepted” as a service to the research community to expedite the dissemination of scientific material as soon as possible after acceptance. “Just Accepted” manuscripts appear in full in PDF format accompanied by an HTML abstract. “Just Accepted” manuscripts have been fully peer reviewed, but should not be considered the official version of record. They are citable by the Digital Object Identifier (DOI®). “Just Accepted” is an optional service offered to authors. Therefore, the “Just Accepted” Web site may not include all articles that will be published in the journal. After a manuscript is technically edited and formatted, it will be removed from the “Just Accepted” Web site and published as an ASAP article. Note that technical editing may introduce minor changes to the manuscript text and/or graphics which could affect content, and all legal disclaimers and ethical guidelines that apply to the journal pertain. ACS cannot be held responsible for errors or consequences arising from the use of information contained in these “Just Accepted” manuscripts.

is published by the American Chemical Society. 1155 Sixteenth Street N.W., Washington, DC 20036

Published by American Chemical Society. Copyright © American Chemical Society. However, no copyright claim is made to original U.S. Government works, or works produced by employees of any Commonwealth realm Crown government in the course of their duties.

Compositions and Formation Mechanisms of Solid-Electrolyte-Interphase (SEI) on Microporous Carbon/Sulfur Cathodes

Luning Wang[†], Yuxiao Lin[#], Samantha DeCarlo[†], Yi Wang[†], Kevin Leung[ǁ], Yue Qi[#], Kang Xu[‡,*], Chunsheng Wang[†,§,*], Bryan W. Eichhorn[†,*]

[†] *Department of Chemistry and Biochemistry, University of Maryland, College Park, MD, 20742, USA.*

[#] *Department of Chemical Engineering and Materials Science, Michigan State University, East Lansing, Michigan 48824, USA.*

[ǁ] *Sandia National Laboratory, Albuquerque, NM 87185, USA.*

[‡] *Electrochemistry Branch, Power and Energy Division Sensor and Electron Devices Directorate, U.S. Army Research Laboratory, Adelphi, MD, 20783, USA.*

[§] *Department of Chemical and Biomolecular Engineering, University of Maryland, College Park, MD, 20742, USA.*

ABSTRACT

We report the formation mechanism and compositions of the solid-electrolyte-interphase (SEI) on a microporous carbon/sulfur (MC/S) cathode in Li-S batteries using carbonate-based electrolyte (1M $LiPF_6$ in ethylene carbonate (EC) / dimethyl carbonate (DMC), v: v = 1: 1). Through characterizations using 1D and 2D solution-phase nuclear magnetic resonance (NMR) spectroscopy, coupled with model chemical reactions and density functional theory (DFT) calculations, we have identified two critical roles of Li^+ in steering the SEI formation. First, the preferential solvation of Li^+ by EC in the mixed carbonate electrolyte renders EC as the dominant participant in SEI formation, and second, Li^+ coordination to the EC carbonyl alters activation barriers and changes the reaction pathways relative to Na^+. The main organic components in the SEI are identified as lithium ethylene mono-carbonate (LEMC) and lithium methyl carbonate (LMC), which are virtually identical to those formed on Li and graphite anodes of lithium ion batteries but via a different pathway.

INTRODUCTION

Lithium-sulfur (Li-S) batteries are of significant interest due to their potential in high energy density (a theoretical value of 2600 Wh/Kg) coupled with the abundance, low-cost and non-toxicity of sulfur.[1-6] The main electrolytes used in Li-S batteries employ ethereal solvents,[6, 7] such as 1,3-dioxolane and 1,2-dimethoxyethane, in contrast to the carbonate-based electrolytes used in commercialized Li-ion batteries.[8, 9] The ether-based electrolytes are adopted to avoid "parasitic reactions" that occur between discharged sulfur species and carbonate molecules.[4, 10, 11] These parasitic processes result in significant sulfur loss[10-12] and incessant solid-electrolyte-interphase (SEI) formation on the cathode surfaces.[12-15] Effective approaches to mitigate these undesired reactions between sulfur and carbonates and the associated capacity losses have been elusive and, as such, much of the Li-S battery research is confined to ether electrolytes, whose sulfide "shuttling" problems have caused concerns for the Li-S full batteries.[2, 16]

The reaction between discharged sulfur cathodes and carbonate solvents, as is indicated by our previous work,[12] turns out to be a double-edged sword. While it induces irreversible capacity loss in the first few battery cycles, it also leads to the generation of SEI, which passivates the sulfur cathode surface and prevents further degradation reactions.[12-15] The battery reported in our previous work survived over 4000 cycles with nearly 100% coulombic efficiency without noticeable capacity degradation after the initial formation of the SEI.[12] The highly stable electrochemical performance based on the similar battery designs has also been reported in other studies.[15, 17-31] Figure 1 shows the electrochemical performance of the Li-S battery that employs a microporous carbon/sulfur (MC/S) composite cathode, where sulfur molecules are trapped in microporous carbon, with 1M $LiPF_6$ in ethylene carbonate (EC) / dimethyl carbonate (DMC) as an electrolyte (Coulombic efficiency data in Figure S1). The specific capacity was calculated based on the mass of all materials on the current collector, which included the MC/S composite, carbon black and binder (Na alginate) in a mass ratio of 70:15:15. In addition to superior cycling stability, the battery displays two distinct features: 1) Single charge and discharge plateaus observed at *ca*. 1.9 V and 1.7 V, respectively, and 2) a precipitous capacity loss in the first discharge process. Whereas several other theories exist to explain the electrochemical features,[13] our previous work indicated that the 1.7 V plateau was due to reduction of small sulfur molecules (*e.g.* S_2) that are trapped in the microporous structure and sealed by SEI, while the capacity loss after the 1st discharge was a result of SEI formation.[12] Chemical/physical characterizations (CO_2 adsorption isotherm, thermogravimetric analysis, X-ray photoelectron spectroscopy, X-ray diffraction (XRD), etc.) and morphological analysis on the microporous carbon and / or the MC/S composite have been detailed in the previous publication as well.[12]

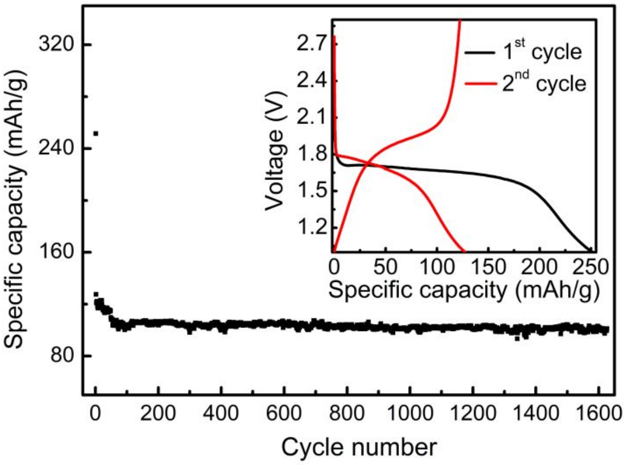

Figure 1. Cycling stability of the Li-S battery fabricated from the MC/S composite. The inset shows the 1st and 2nd electrochemical cycles. The specific capacity is calculated based on the mass of all materials on current collector.

The importance of the SEI in the stable performance of Li-based anodes (graphite, Li metal, *etc.*) has been widely recognized.[8, 32-34] Historically the failure to comprehend the role of SEI has caused significant delay in the development of Li-ion batteries.[35] In our previous work, we have rectified a general misidentification of a major organic species in the SEI generated on graphitic anode in a typical carbonate electrolyte (1M $LiPF_6$ in EC/DMC). The organic components are identified to be lithium ethylene mono-carbonate (LEMC, Figure 2) and lithium methyl carbonate (LMC, Figure 2), instead of the widely accepted lithium ethylene di-carbonate (LEDC, Figure 2).[36]

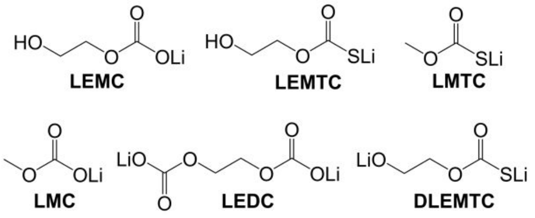

Figure 2. Molecular structures of lithium ethylene mono-carbonate (LEMC), lithium ethylene mono-thiocarbonate (LEMTC), lithium methyl thiocarbonate (LMTC), lithium methyl carbonate (LMC), lithium ethylene di-carbonate (LEDC) and di-lithium ethylene mono-thiocarbonate (DLEMTC).

In contrast to Li-based anodes, SEI (or sometimes known as the cathode-electrolyte-interphase, CEI) on cathodes has been much less studied. When carbonate electrolytes are used in the Li-S battery systems, it is generally accepted that SEI layers are formed on the sulfur-based cathodes resulting from reactions between discharged sulfur species and the carbonate solvents.[12, 13, 15, 24, 37] The reactivity of highly nucleophilic sulfides towards electrophilic sites in carbonates[10, 11] and the observation of large irreversible capacity loss in the initial few battery cycles provide evidence for SEI formation on sulfur cathodes.[12, 13, 15, 37] Scanning electron microscopy (SEM), energy-dispersive spectroscopy (EDS), electrochemical impedance spectroscopy (EIS) and X-ray photoelectron spectroscopy (XPS) have been employed to identify the general compositions and morphologies of the SEI.[12, 14, 15, 37] Specifically, researchers have recognized the important role of "quasi-solid-state" behavior of sulfur species in describing the single plateau feature in Li-S batteries.[14, 15, 26, 37] However, the specific chemical compositions, mechanism of formation and hierarchical structure of such unique SEI layers remain largely unknown.

Herein, we identify the specific chemical compounds present in the SEI on sulfur cathodes and their formation mechanisms in the Li-S batteries. Through the use of 1D and 2D NMR spectroscopy coupled with model chemical reactions and direct analysis of SEI layers, we describe the critical role of Li^+ coordination to EC in directing the chemical routes of SEI formation. Our work demonstrates that the SEI layer on the sulfur cathode contains the same organic components (*i.e.*, LEMC + LMC) as those on the graphite anode reported elsewhere,[36] but are formed by completely different chemical mechanisms. A model for the SEI formation is suggested, where an electrochemical double layer (EDL) is generated on the surface of sulfur cathodes prior to the irreversible reaction between sulfide and carbonate. DFT studies show that Li^+ coordination to the EC carbonyl alters the activation barriers and changes the reaction pathway in the presence of Li^+ versus Na^+. Unravelling the composition of the SEI components on the sulfur based cathodes opens up new opportunities for artificial SEIs that could significantly reduce / eliminate the initial capacity losses associated with SEI formation while completely eliminating parasitic sulfur shuttling. In addition, the unexpected link between Li/C anode SEI films and the sulfur cathode SEI films described here opens up new possibilities for single-component thin films that serve as both solid-state electrolyte and SEI.

EXPERIMENTAL SECTION

General regents and instruments. All regents were purchased from commercial resources (Sigma-Aldrich, Cambridge Isotope Laboratories Inc., Fisher Scientific, MP Biomedicals, Alfa Aesar) unless otherwise stated. Sure/Seal anhydrous methanol and ethylene glycol were purchased from Sigma-Aldrich and used without further purification. Prior to use, DMSO-*d*$_6$ (99.9%) and Sure/Seal anhydrous DMC were dried by activated 4A molecular sieves for at least 72 h. Acetonitrile, pyridine and DMSO were distilled over CaH_2. Diethyl ether and THF were distilled over Na benzophenone. $LiPF_6$ was dried under vacuum in a Schlenk line for 12 h at 50 ^oC.

NMR spectra were recorded on Bruker AV-400 MHz, Bruker DRX-500 MHz, or Bruker Ascend 800 MHz high resolution spectrometers. All NMR spectra collected in DMSO-*d*$_6$ were referenced to DMSO-*d*$_6$ at 2.500 ppm for ^1H NMR and 39.52 ppm for ^{13}C NMR. ^1H NMR spectra collected in D_2O were referenced to EC at 4.500 ppm. NMR Chemical shifts (δ) were reported in ppm and multiplicities were indicated by s (singlet), d (doublet), t (triplet), q (quartet), m (multiplet) and br (broad). Coupling constants *J* were reported in Hertz (Hz). X-Ray diffraction (XRD) patterns were collected on a Bruker C2 spectrometer, with all samples sealed in 0.5 mm capillaries under Argon. FTIR measurements was carried out employing a Thermo Nicolet 670 spectrometer. Samples for FTIR measurements were sealed in a diffuse reflectance (DRIFTS) cell under Argon. Battery and electrochemical tests were carried out in either a button cell (CR2032) in a Landit electrochemical test station, or in a swagelock/beaker cell using a Wavenow USB Potentiostat in an Ar-filled glovebox. ESI-MS was performed on a JEOL AccuTOF-CS mass spectrometer. More experimental details on ESI-MS are in the supporting information.

SEI functionality revealed by H_2O extraction. Unless otherwise stated, all sulfur cathodes were cycled using 1M $LiPF_6$ in EC/DMC (v: v = 1: 1) as the electrolyte and Li metal as the counter electrode. The sucrose-derived microporous carbon, the MC/S composite and round ½ inch (in diameter) cathodes of MC/S were fabricated by following the procedure reported by Xu et al.[12] Additional details of the cell design are given in Supporting Information. The cathodes were cycled three times from 1.0 to 3.0 V in a Swagelock cell and recovered at their charged states. Afterwards, the electrodes were carefully rinsed with DMC three times in a glovebox, or by 0.1 M HCl aqueous solutions for 1 min in the air. The HCl rinse electrode was extensively dried under vacuum overnight at 60 ^oC to remove residual moisture before being re-assembled into Swagelock cells for further electrochemical measurements.

Extraction and analysis of Cathode SEI layers. To generate sufficient SEI materials for analysis, large-area sulfur cathodes (~ 100 cm^2), containing ~ 50 - 100 mg MC/S composites (Cathode MC/S) were fabricated. As a reference, a sulfur-free microporous carbon cathode (Cathode MC), which only contained microporous carbon, carbon black and binder, was also fabricated. Details regarding the fabrication of cathodes are in the Supporting Information. All large-area cathodes were cycled between 1.4 to 3.0 V in a beaker in an Ar-filled glovebox. After cycling at least three times, the cathodes were recovered at their charged states and rinsed with anhydrous DMC or acetonitrile. The electrodes were dried under vacuum for 12 h, immersed in ~ 2 ml DMSO-d_6 for 3 h, or ~ 2 ml 0.1 M DCl in D_2O for 60 s to dissolve the SEI components.

Chemical synthesis and model chemical reactions. All experimental procedures were carried out under inert atmosphere using Schlenk line techniques or in an Ar-filled glovebox. Details on the synthesis of lithium ethylene glycolate ($LiOCH_2CH_2OH$) and lithium tert-butoxide (LiOtBu) are in the Supporting Information.

1) Synthesis of LMTC. Carbonyl sulfide gas (COS) was synthesized through the reaction of KSCN and H_2SO_4 following literature protocols (see SI for details).[65-66] To a stirred solution of anhydrous methanol (20 ml) at 0 ^oC was added 2.5 M n-BuLi/hexane solution (10 ml, 25 mmol) dropwise. The reaction was warmed to room temperature and further stirred for an additional 30 min. Afterwards COS gas was bubbled through the CH_3OLi/MeOH solution for 3 h using a gas infuser. The reaction was exothermic. The methanol solvent was removed *in vacuo* at room temperature yielding a highly viscous LMTC/MeOH solution. The viscous solution was rinsed repeatedly with anhydrous diethyl ether, and subsequently dried *in vacuo* for 48 h to obtain a light-yellow powder of LMTC (1.86 g, yield 76% based on

n-BuLi). ^{1}H NMR (500 MHz, DMSO-d_6) δ 3.270 (s). ^{13}C NMR (126 MHz, DMSO-d_6) δ 183.32, 51.07; IR (KBr, DRIFTS) 2995, 2946, 2849, 2795, 1672, 1491, 1439, 1378, 1201, 1128, 1059, 830, 735, 690 cm^{-1}. HRMS (ESI) *m/z*: $[LMTC - Li]^-$ Calcd for $C_2H_3O_2S^-$ 90.9854, found 90.9561.

2) Synthesis of LEMTC. Lithium ethylene glycolate $LiOCH_2CH_2OH$ (300 mg, 4.4 mmol) was suspended in anhydrous CH_3CN (15 ml). $COS_{(g)}$ was bubbled through the vigorously stirred suspension for 3 h, during which time period the white suspension gradually turned light yellow in color. The CH_3CN solvent was removed *in vacuo* to obtain a light-yellow powder of LEMTC (462 mg, yield 82% based on $LiOCH_2CH_2OH$). ^{1}H NMR (600 MHz, DMSO-d_6) δ 4.603 (s), 3.779 (s), 3.744 (t, *J* = 5.8 Hz), 3.416 (t, *J* = 5.8 Hz), 3.364 (s). ^{13}C NMR (151 MHz, DMSO-d_6) δ 183.47, 183.27, 65.71, 62.91, 62.85, 60.10. IR (KBr, DRIFTS) 3305, 2966, 2928, 2875, 1644, 1522, 1456, 1401, 1360, 1314, 1254, 1223, 1166, 1073, 925, 889, 825, 724, 684 cm^{-1}. HRMS (ESI) *m/z*: $[LEMTC - Li]^-$ Calcd for $C3H5O3S^-$ 120.9959, found 120.9762.

3) Synthesis of DLEMTC · *x* DMSO. LEMTC (220mg, 1.72 mmol) was dissolved in anhydrous DMSO (5 ml) to give a yellow solution, followed by the addition of lithium tert-butoxide (150 mg, 1.87 mmol, 1.1 equiv.) and stirred for 2 h. Anhydrous THF (40 ml) was subsequently added, which instantly generated a white precipitate. After the suspension was stirred for 3 h, the precipitate was collected by centrifugation, rinsed with anhydrous THF and dried *in vacuo*. NMR studies showed the powder to contain primarily DLEMTC · *x* DMSO (x ~ 5) with small amounts of LEDTC (10 – 30 %). White/light yellow powder, 78 mg. ^{1}H NMR (500 MHz, DMSO-d_6) δ 3.748 (t, *J* = 6.0 Hz), 3.421 (t, *J* = 5.8 Hz). ^{13}C NMR (126 MHz, DMSO-d_6) δ 183.20, 65.32, 59.94.

4) Chemical reactions of Li_2S with EC and/or DMC. All reactions were conducted in a glovebox filled with Ar at room temperature. To stirred solutions of 1M $LiPF_6$ in EC/DMC (v: v = 1: 1, 2 g), or 1M $LiPF_6$ in EC (152 mg $LiPF_6$ + 1.3 g EC) was added finely ground Li_2S powder (50 - 100 mg) to give white-colored suspensions. The reactions were allowed to stir for *ca.* 1 week, after which the precipitates in the suspensions were isolated by centrifugation, rinsed with anhydrous DMC (for EC/DMC reaction) or anhydrous acetonitrile (for EC reaction), dried under vacuum for 12 h and dissolved in D_2O or extracted into DMSO-d_6 for NMR analysis. Additional details are given in the SI.

5) Chemical reactions of thiocarbonates with EC and/or DMC. To a vial charged with a stirred solution of 1M $LiPF_6$ in EC/DMC (v: v = 1: 1, 1.0 – 2.0 g), 1M $LiPF_6$ in DMC (1.0 – 2.0 g), or 1M $LiPF_6$ in EC (152 mg $LiPF_6$ + 1.3 g EC) was added LMTC (50 mg, 0.50 mmol), LEMTC (64 - 100 mg, 0.50 – 0.78 mmol) or DLEMTC · *x* DMSO (20 – 30 mg). The thiocarbonates showed little to moderate solubilities in the carbonate solutions. The reactions were allowed to stir for 15 - 48 h, the precipitates collected by centrifuge, rinsed by anhydrous CH_3CN, dried under vacuum and dissolved/extracted into DMSO-d_6 for NMR analysis. Reaction supernatants were also analyzed by NMR spectroscopy. Additional details are given in the SI.

Theoretical Simulations. DFT calculations were performed to determine the reaction barriers and energy changes associated with the reactions between EC and two sulfur containing species: Li_2S and Na_2S. Various reaction paths were constructed and compared, with the use of two sets of DFT functionals, software, and solvation model protocols to cross-check the predictions. One applied the G09 suite of programs,[39] the PBE0 functional,[67-68] a 6-31+G(d,p) basis, and the SMD solvation model[69] with a dielectric constant of 70. The simulation cell contains either one or five EC molecules and the sulfur species. If five EC molecules are present, optimization was performed using the 6-31G(*) basis followed by a 6-31+(d,p) single point energy calculation; otherwise 6-31+G(d,p) was used throughout. The vibrational frequencies were computed using harmonic analysis, and finite temperature entropy contributions were added to the energies predicted. The other set of calculations applied DMOL3 implemented in Materials Studio,[40] PW91,[70] and COSMO solvation method[71] with a dielectric constant of 70. PBE0 generally predicts higher reaction barriers than PW91, therefore comparing the two sets of predictions gives important trends regarding the accuracy of predicted barriers. Additional computational details are given in the Supporting Information.

Results

SEI functionality revealed by H_2O extraction. The importance of the SEI on the MC/S cathode performance and the impact of SEI formation on capacity are evidenced in the initial charge-discharge cycles of the Li-S battery. The electrochemical experiments in Figure 3 show that the SEI allows Li^+ ion transport but prevents the confined sulfur in the microporous carbon from reacting with the carbonate electrolytes. This functionality is illustrated by cycling the MC/S cathodes in Li-S batteries with and without the protective SEI layer. To accomplish this task, we removed the SEI from a pre-cycled MC/S cathode (3 cycles) by rinsing the cathode with 0.1 M HCl aqueous solution and compared the electrochemical behavior before and after the rinse. During the rinse of the cathode in its charged state, care was taken to avoid the loss of active materials. After the HCl rinse, residual water from the extraction process was removed under extensive vacuum. A control experiment employing a rinse with anhydrous DMC was also conducted for comparison. For simplicity, the capacities for all electrodes are normalized to their capacities before rinsing. The black curves in both figures demonstrate typical discharge characteristics for a MC/S cathode with a single discharge plateau at ~ 1.7 V. The red curves in Figure 3a display charge and discharge plateaus after the electrode is rinsed with dry DMC solvent. As expected, due to the insolubility of the SEI in DMC, the rinse does not affect the cycling behavior. However, rinsing the MC/S cathode with 0.1 M HCl aqueous solution leads to major changes in MC/S cathode behavior. The previous discharge plateau at *ca*. 1.7 V is missing and, in its place, a substantially lower plateau at *ca.* 1.3 V is observed (blue curve in Figure 3b) while the overall capacity is maintained. The subsequent charge process shows a large capacity loss (*ca*. 70%). We attribute this observation to the following chemistry. After the pre-formed SEI is removed by the HCl rinse, the active sulfur material (elemental sulfur in the charged state) is completely exposed to electrolyte when the cell is reconstituted. The lithium sulfides formed during subsequent battery discharge can now react with carbonate molecules and generate new SEI coverage. In this process, the sulfide anions are transformed into SEI components that are electrochemically deactivated in the following battery cycles, as is evidenced by the additional precipitous capacity drop.

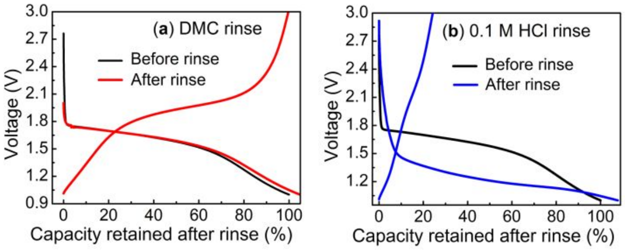

Figure 3. Battery cycling performance after the cycled cathodes are rinsed by (a) DMC and (b) 0.1 M HCl aqueous solutions. The black curves in both figures show a typical discharge behavior of SEI-protected cathode. Capacities of all cathodes are normalized to the capacities before rinse.

To determine the identity of the chemical components and reveal the mechanism of SEI formation, we have extracted the SEI layer components into deuterated dimethyl sulfoxide (DMSO-d_6) and D_2O and performed 1D and 2D NMR spectroscopic measurements. In addition, we also synthesized authentic model compounds to reveal the reactivities and identities of the molecular components present in the SEI. Studies on the model chemical systems are described first.

Reactions of Li_2S with EC/DMC. Previous studies on the parasitic reactions of sulfides with carbonate-based electrolytes have focused on the reactivity of polysulfides S_x^{2-} (where x > 1), which undergo nucleophilic addition to a carbonyl carbon (Path A in Scheme 1, red arrows),[11] or an alkyl carbon (Path B of Scheme 1, blue arrows) of the carbonate molecules.[10] The reactivity of monosulfides (*e.g.*, Li_2S), however, is much less understood, perhaps due to their limited solubility in common aprotic solvents including EC/DMC. Our investigation shows that the reactions of S^{2-} with EC and DMC *can* follow Path A or Path B depending on which cation species (Li^+ *vs.* Na^+) is present in the electrolyte. Reactions of Li_2S with EC and DMC primarily follow Path A chemistry, generating intermediate compounds di-lithium ethylene mono-thiocarbonate (DLEMTC, Figure 2) and lithium methyl thiocarbonate (LMTC, Figure 2), respectively (Scheme 1). These intermediates are not stable in EC and / or DMC, and react with the carbonate solvents to give LEMC or LMC as the final products (Scheme 1). In our model systems, we assume that LiS^- is the initial sulfide nucleophile in reactions with the carbonates as it is the first ionization product formed from Li_2S dissociation ($Li_2S \rightleftharpoons Li^+ + LiS^-$) and bare S^{2-} is too highly charged and reactive to stably exist in solution. We cannot exclude molecular Li_2S complexes or heterogeneous reactions as initial steps of the process. However, experimental data suggest that Li^+ and LiS^- are the reactive species. Molecular simulations demonstrate the importance of Li^+-EC coordination in steering the chemical routes.

Because the SEI by definition is insoluble in electrolyte solutions, our model systems focused on the insoluble precipitates formed in chemical reactions between sulfur nucleophiles and carbonate solvents. The analysis of the soluble components is given in the supporting information (Figure S2). In a typical reaction, finely ground powders of Li_2S were added to the corresponding carbonate solvents and stirred for several days at room temperature in an Ar-filled glovebox. The insoluble precipitates were isolated, rinsed with anhydrous acetonitrile / DMC, extracted into DMSO-d_6 and evaluated by ^1H NMR spectroscopy (Figure 4). The reaction products and pathways are given in Scheme 1. Product identifications were made through comparisons with authentic standards whenever possible.

Scheme 1. Path A and Path B of EC and DMC reacting with Li_2S.

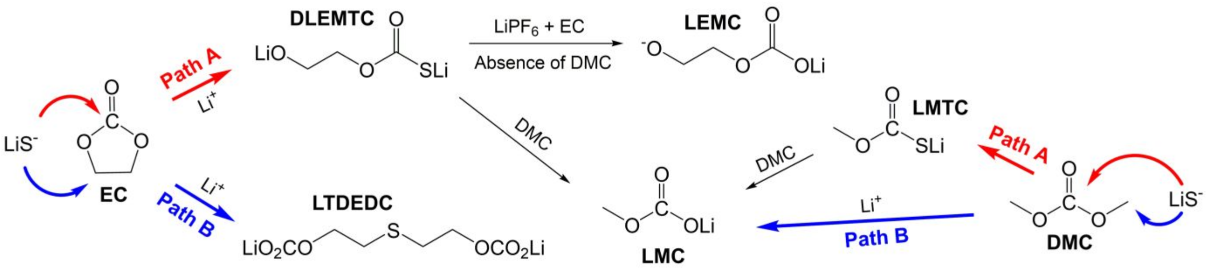

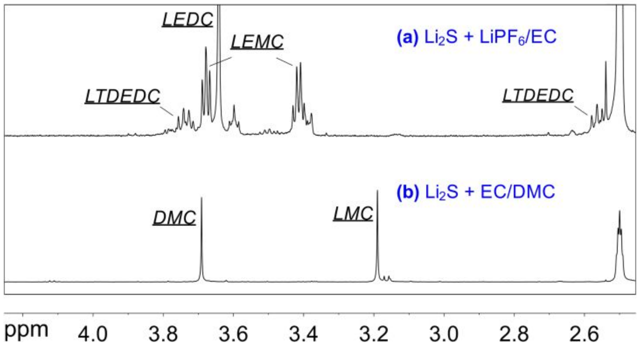

Figure 4. ^1H NMR spectra (DMSO-d_6, 25 °C) of the precipitates from model chemical reactions of (a) Li_2S with $LiPF_6$/EC and (b) Li_2S with EC/DMC (v: v = 1: 1). Spectra (a) and (b) were collected at 500 MHz and 400 MHz, respectively.

The reaction of Li_2S with the solvent mixture EC/DMC yields LMC as the major product (Figure 4b and Figure S3), while the reaction with EC (in absence of DMC) generates LEMC (Figure 4a). The presence of LEDC observed in the NMR studies (Figure 4a) results from a secondary equilibrium reaction that occurs when LEMC is extracted into DMSO-d_6 for NMR studies (*i.e.* the chemical reaction of Li_2S and EC does *not* give LEDC). This equilibrium relationship has been discussed in detail in a previous publication[36] and shown in eq (1) below. In the next section, we discuss the formation mechanisms of these products (LEMC and LMC) through chemical synthesis of Path A intermediates.

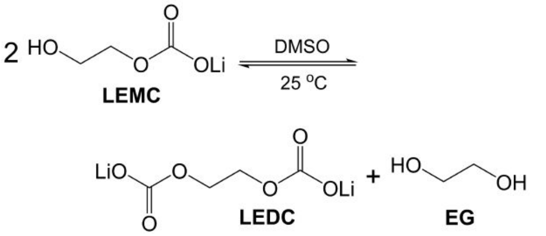

(1)

Scheme 2. Synthesis of (a) LEMTC and DLEMTC · *x* DMSO and (b) LMTC.

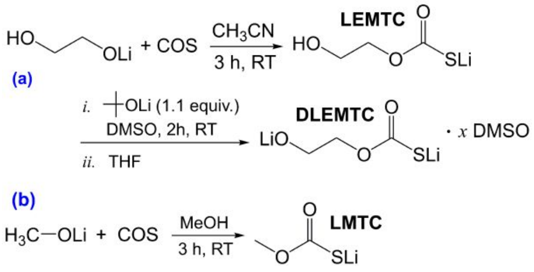

The syntheses of the thiocarbonate intermediates (*i.e.*, LMTC, LEMTC and DLEMTC) were accomplished by nucleophilic addition of alkoxides to carbonyl sulfide (COS) gas (Scheme 2). Specifically, $LiOCH_3/CH_3OH$ solutions react with COS to generate LMTC dissolved in CH_3OH. Removal of the solvent under vacuum gives a white/light-yellow polycrystalline powder LMTC in 76% yield (Scheme 2b). Likewise, $LiOCH_2CH_2OH$/acetonitrile suspensions react with COS to give LEMTC as a light-yellow polycrystalline solid in 82% yield (Scheme 2a). Characterization data for the thiocarbonate compounds (solution NMR, Fourier-transform infrared (FTIR), electrospray ionization mass spectroscopy (ESI-MS) and powder XRD) are given in the experimental section and in the Supporting Information (Figure S4 – S9). The compounds are air / moisture sensitive and react with protic solvents and impurities. LMTC and LEMTC are soluble in anhydrous DMSO, dimethylformamide (DMF) and pyridine. In all the three aprotic solvents (*i.e.*, DMSO, DMF and pyridine), LEMTC disproportionates into lithium ethylene di-thiocarbonate (LEDTC) and ethylene glycol (EG) according to eq 2, which is similar to the equilibrium behavior of LEMC previously described (eq 1 above).[36] The NMR data were collected from analytically-pure LEMTC and all LEDTC and EG observed in the NMR analyses (Fig. S4) are generated through the disproportionation reaction (*i.e.* LEDTC and EG are not present in the powder samples). Deprotonation of LEMTC by lithium *tert*-butoxide in DMSO generates DLEMTC· *x* DMSO (Scheme 2a), which can be precipitated from solution upon addition of tetrahydrofuran (THF). However, the THF addition always leads to the co-precipitation of DLEMTC · x DMSO together with *ca.* 10 – 30 % LEDTC due to the equilibrium established in DMSO solutions (eq 2). Currently, we are unable to obtain pure DLEMTC and the synthesized powder mixture is amorphous (Figure S7).

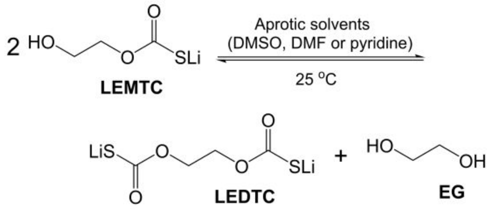

(2)

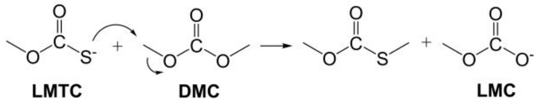

(3)

In all cases, LMTC, LEMTC and DLEMTC react with EC or DMC to give their sulfur-free carbonate analogs (LEMC and LMC). The reaction results are summarized in Table 1, Scheme 1 and Figure S10 – S15. DMC dominates these reactions to generate LMC whenever present. In the absence of DMC, DLEMTC reacts with $LiPF_6$/EC to form LEMC. ^1H and ^{13}C NMR studies on the DMC reactions suggest a mechanism proceeds through nucleophilic addition of thiocarbonate anions to DMC alkyl carbons (eq 3 and Figure S11 - S15). The EC reaction, on the other hand, seems to proceed through a nucleophilic addition of alkoxide to the EC carbonyl, followed by a secondary nucleophilic addition (Figure S10). Similar reactions of LiOMe with EC have been previously reported.[36, 38]

The above results of thiocarbonate reactivities indicate that the reactions of Li_2S very *likely* follow Path A chemistry (Scheme 1). DLEMTC is indeed generated as an intermediate in the reaction of Li_2S with EC (in the absence of DMC), but is subsequently consumed to yield LEMC as the final product (Figure 4a). When DMC is present in the reaction, as is the case of Figure 4b, all Path A intermediate products (DLEMTC, LEMTC and LMTC) *preferentially* react with DMC to give LMC as the only product.

The reaction of Li_2S with EC in 1M $LiPF_6$ (Figure 4a) shows a minor path B product, lithium thiodiethylene di-carbonate (LTDEDC, Scheme 1). The proposed mechanism for LTDEDC formation is nucleophilic addition of S^{2-} to alkyl carbons of the EC that is *uncoordinated* by Li^+ in the 1M solution. This reaction acts as a competing process with Path A that is catalyzed by the Li^+ coordination to EC. The analysis is based on the molecular simulations (see below) in comparisons with corresponding Na^+ electrolytes, where we demonstrate the critical role of cation-EC coordination in steering the preferred chemical route.

Table 1. Summary of the reactions of thiocarbonates with EC/DMC.

Reactant (powder)	Reactant (liquid solution)	Reaction time/h	Products
LEMTC	1M $LiPF_6$ in EC/DMC	24	LMC
LEMTC	1M $LiPF_6$ in DMC	24	LMC
LMTC	1M $LiPF_6$ in DMC	24	LMC
LMTC	1M $LiPF_6$ in EC/DMC	15	LMC
DLEMTC	1M $LiPF_6$ EC/DMC	24	LMC
DLEMTC	1M $LiPF_6$ DMC	48	LMC
DLEMTC	1M $LiPF_6$ in EC*	48	LEMC

* Mixture of 152 mg $LiPF_6$ with 1.3 g EC forms a clear solution at ~ 26 ^{o}C in an Ar-filled glovebox.

Theoretical simulations. Molecular simulations were performed to gain a better understanding of the reactions between Li_2S and EC. Reactivities of Na_2S were also investigated to illustrate the influences of different cation species. Two different computational methods were applied, which give similar results consistent with our experimental observations. The inclusion of additional solvent molecules in the Gaussian 09 (G09) simulations[39] provides more accurate analysis of activation barriers and reaction energy changes resulting in the reaction profiles in Figure 5b, while the lower number of solvent molecules in the DMOL3 simulations[40] enables the calculation of transition state structures (Figure 6). Additional details on simulations are described in the Supporting Information (Figure S23-S26, Table S1). To maintain charge balance and a neutral starting point, our simulations employ Li_2S (and Na_2S) as the initial reactants for reactions with the organic carbonates. These molecular salts ionize into Li^+ and LiS^- (or Na^+ and NaS^-) during the early stage of reaction. In solution, the ionized species (Li^+ and LiS^-) may be the intial reactants but both approaches give the same endpoints.

The main conclusions of the computational studies are as follows: (1) For the reaction of EC with Li_2S and Na_2S, both path A and B are exothermic, with path B thermodynamically favored in all cases. However, the lower activation barriers make path A kinetically favored in all cases. (2) For path A reactions, the presence of Li^+ leads to a lower energy barrier than Na^+. The calculated activation energies for the Li^+ reactions are solvent dependent with the G09 simulation giving a small 0.27 eV barrier (Figure 5b) whereas the DMOL3 simulation was almost barrierless (0.05 ev, Figure 5a). A detailed examination of the molecular configurations on the transition states (Figure 6) indicates a much stronger Li-O interaction with the carbonyl group (Li-O distance 1.933 Å) than the sodium case (Na-O distance 3.393 Å). The strong coordination of Li^+ to O enables a resonance stabilized transition state that lowers the reaction barrier of Path A. In contrast, Path B reactions for both Na^+ and Li^+ have quite similar activation barriers (~ 0.6 eV) and transition state geometries (Figure 6). These data suggest that the presence of Li^+ ions in solution will promote Path A chemistry over Path B chemistry, which is consistent with experimental observations. While the Path A activation energy for Na_2S is larger than that of Li_2S, the ΔE_{rxn} is much *smaller* for Na_2S (-0.43 eV) than for Li_2S (-0.92

eV) (Figure 5b). The Path A reaction for Na_2S should be reversible at room temperatures whereas the -0.92 eV exothermicity for the Li_2S reaction renders it irreversible. This finding suggests that while Path A is kinetically favored in reactions of Na_2S with EC, the reversibility of the Path A reaction in the Na_2S system facilitates the accumulation of the thermodynamically favored Path B products. These findings are consistent with the experimental results that show the exclusive formation of Path A products in SEIs generated in the presence of Li^+ ions (See below). In contrast, SEIs formed from Na^+-derived electrolytes give large fractions of Path B products, as is outlined in the Supporting Information (Figure S16) and will be described in a subsequent publication.

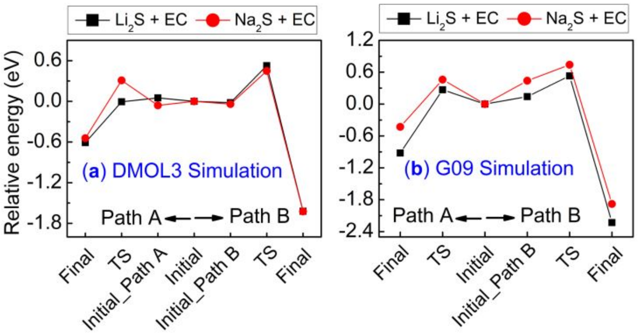

Figure 5. Relative energy of reactions of (black) Li_2S + EC and (red) Na_2S + EC in different reaction states calculated with (a) DMOL3 and (b) G09 simulations.

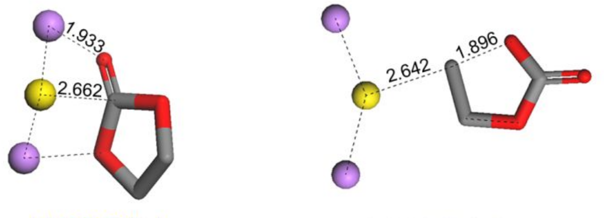

(a) Li_2S, Path A (b) Li_2S, Path B

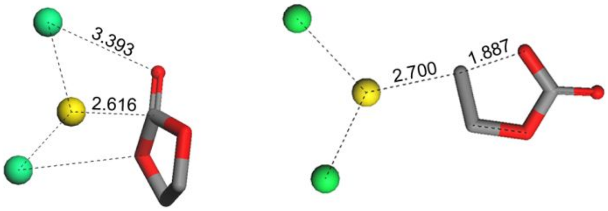

(c) Na_2S, Path A (d) Na_2S, Path B

Figure 6. Transition states (DMOL3 simulations) for Path A and Path B of EC reacting with Li_2S and Na_2S.

Compositions of SEI layers in Li-S batteries. Determining the chemical composition of authentic SEIs is of high importance but difficult due to their nanometer-scale thickness, insolubility, amorphous nature, and high sensitivity to air and moisture.[8, 33, 41] Various techniques have been employed to characterize SEI layers on different electrodes, such as FTIR, XPS, Raman and solid-state NMR spectroscopy.[34, 41-54] While these studies provide valuable insight into the functional groups present in the SEI layers, the identity of the specific chemical compounds is difficult to ascertain by these methods. To yield precise chemical structures of SEI components, we resorted to solution-phase 1D and 2D NMR spectroscopy, which were conducted by extracting SEIs into DMSO-*d*$_6$ or 0.1M DCl/D_2O (Figure 7). To ensure sufficient quantities of SEI compounds were generated on the cathode surface, we fabricated large cathodes (~ 100 cm^2) from sulfur-free, bare microporous carbon (Cathode MC) and the MC/S composite (Cathode MC/S). Two types of electrolytes were used, namely 1M $LiPF_6$ in EC/DMC (v: v = 1: 1) and 1M $LiPF_6$ in neat EC. The cathodes were cycled *vs.* Li from 1.4 to 3.0 V to generate SEIs and the electrochemical data are shown in Figure S17. As expected, the sulfur-free Cathode MC shows very limited capacity and no sulfur-based plateau (Figure S17a). This observation shows that the electrolyte, 1M $LiPF_6$ in EC/DMC, is electrochemically stable in the voltage range, which agrees well with previous studies.[55] Figure S17b shows electrochemical performance (1st and 2nd discharge and charge processes) of Cathode MC/S in a Li-S battery, which is similar to Figure 1, but with much higher total capacity. The large difference in specific capacity between the MC/S cathode and the blank MC cathode (Figure S17 a and b) indicates that the Li storage capacity of the MC/S cathode almost entirely originates from sulfur redox and not from the carbon support.

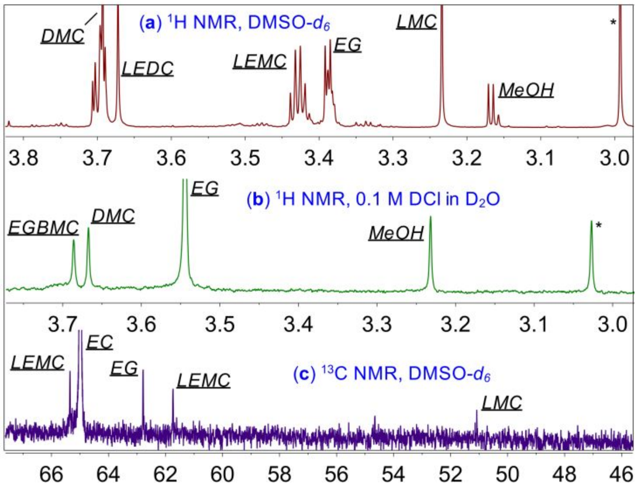

Figure 7. ^{1}H NMR spectra of SEI layer from Cathode MC/S extracted into (a) anhydrous DMSO-*d*$_6$ and (b) 0.1 M DCl in D_2O. (c) ^{13}C NMR spectra of SEI layer on Cathode MC/S extracted into anhydrous DMSO-*d*$_6$. EGBMC: ethylene glycol bis(methyl carbonate). * Unidentified peaks. Spectra (a) and (c) were collected at an 800 MHz NMR spectrometer while (b) at 500 MHz at 25 °C.

After cycling at least 3 times, the cathodes were recovered in their charged state, the soluble components (*e.g.*, residual EC and $LiPF_6$) removed via a DMC or acetonitrile rinse, dried under vacuum and the insoluble SEI components extracted into DMSO-d_6 and D_2O for NMR analysis. As a control experiment, Figure S18 shows the ^1H NMR spectrum of the SEI extraction for the sulfur-free Cathode MC. Only residual EC is observed in the spectrum without any sign of solvent decomposition, indicating that the electrolytes are electrochemically stable in the voltage range of 1.4 V to 3.0 V, consistent with prior knowledge of EC/DMC electrolytes.[55-59]

1D and 2D NMR spectra of DMSO-d_6 and D_2O extractions from cycled Cathode MC/S are shown in Figure 7, Figure S19 and S20. When EC/DMC is used as the electrolyte, NMR spectra of the DMSO-d_6 extraction (Figure 7a) indicate the presence of numerous compounds, including LEMC, LEDC, EG, LMC, ethylene glycol bis(methyl carbonate) (EGBMC) and methanol (MeOH), as well as residual EC and DMC. The identities of these compounds were confirmed through addition of synthetic standards (LEMC and LMC) into the DMSO-d_6 solutions. Moreover, the absence of the thiocarbonates (LEMTC and LMTC) was also confirmed through comparisons with the synthetic standards (Figure S21 and S22). EGBMC is formed through non-electrochemical process, as described elsewhere[38, 59, 60] and in Scheme S1.

Our previous work has revealed complex equilibria/interconversions between these compounds in DMSO solutions, including (1) equilibrium of LEMC with LEDC and EG (Scheme 3a) and (2) reactions of LEMC with DMC to give LMC (Scheme 3b and Scheme S2).[36] These equilibria and interconversions present a significant challenge to the accurate determination of SEI compositions by solution NMR spectroscopy (*i.e*. were the compounds present before DMSO-d_6 extraction). To circumvent this issue, we conducted parallel experiments in which the SEI compounds formed from EC/DMC electrolytes were hydrolyzed in 0.1 M DCl/D_2O solution. The spectrum (Figure 7b) indicates the presence of the alcohols EG and MeOH, which are formed through hydrolysis of LEMC and LMC, respectively (Scheme 3 c and d). We have previously shown that the interconversions observed in DMSO are precluded in the acidic aqueous solution and therefore, the presence of both alcohols indicates that both EC-derived products (*e.g.* LEMC) and DMC-derived products (*e.g.* LMC) exist in the SEI layers on the sulfur cathode.[36] When pure EC (no DMC) is used as the electrolyte solvent, NMR spectra (Figure S19) of the SEI extracts show the presence of LEMC. The observed LEMC most likely comes from reactions of DLEMTC with EC, as is demonstrated in the chemical model experiments described in the previous section (See Table 1). These spectroscopic studies and control experiments strongly suggest that LEMC and LMC are quite *likely* the major organic components in the sulfur cathode SEIs.

Scheme 3. (a, b) equilibria/interconversions of LEMC and (c, d) hydrolysis of LEMC and LMC.

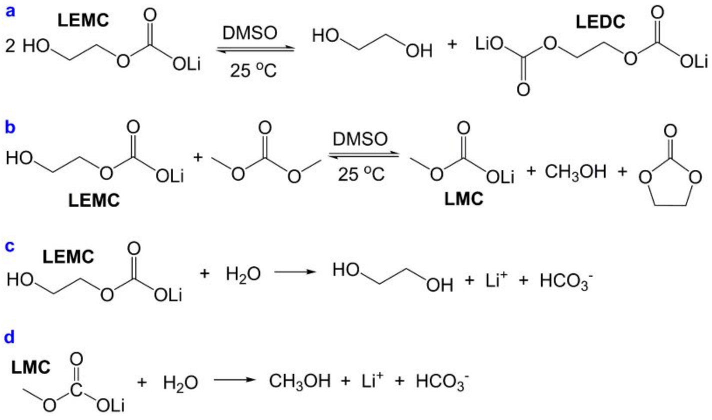

DISCUSSION

Combining the model chemical reactions with the direct analysis of authentic SEIs provides valuable insights into the mechanism of SEI formation on the MC/S cathodes. The presence of LEMC as a major SEI component on Cathode MC/S is suggestive of a highly ordered electrochemical double layer (EDL) at the MC/S cathode-electrolyte interface (Scheme 4). Previous molecular simulations and experimental studies clearly show preferential solvation of Li^+ by cyclic carbonates (e.g., EC) over linear carbonates (e.g., DMC) in binary solvent mixtures (e.g., EC/DMC).[61-65] This solvation preference leads to the formation of $Li^+(EC)_n$ (n = 3-5) complexes as the major species present in EC/DMC electrolyte solutions.[65-67] To balance the negative charges of the sulfides formed in the cathode during cell discharge, the solvated $Li^+(EC)_n$ cations migrate to the MC/S cathode and accumulate at the polarized liquid-solid interface (see Scheme 4). Similarly structured EDLs at polarized electrodes have been proposed in previous studies.[68, 69] This ordering process generates an EC-rich region at the electrode-electrolyte interface and effectively removes DMC from the charged liquid-solid interface, which leads to EC being the primary organic reactant in the SEI formation. The EC at this interface is also activated towards nucleophilic attack due to the coordination to the Li^+ cations.

We attribute the presence of LEMC in the MC/S cathode SEI to a direct result of the highly order EDL. Under such circumstances, the S^{2-} ions formed at the surface of the cathode during the initial discharge would only be exposed to an inner-Helmholtz layer that is heavily populated by Li^+-activated EC molecules. This proposal is based upon the following experimental facts.

(i). Our model chemical reactions indicate that the reactions of Li_2S with the carbonate electrolyte, whenever DMC is present, *always* lead to the formation of LMC as the *exclusive* product. *No* LEMC is detected under these circumstances.

(ii). Similarly, model chemical reactions of carbonate electrolyte with the thiocarbonates (LMTC, LEMTC and DLEMTC), which are the intermediate products from Path A chemistry of Li_2S, also *only* generate LMC whenever DMC is present in the reaction. Again, *no* LEMC is detected.

(***iii***). We can only detect LEMC formation in a DMC-free reaction, as is the case in the reaction of Li_2S + EC (Fig. 4a) and DLEMTC + EC (Fig. S10 and Table 1).

(***iv***). In our SEI extraction experiment, we repeatedly find LEMC as the major SEI component, even when there is equal volume quantities of DMC in the electrolyte (EC: DMC = 1:1, v: v). Since our model chemical systems in (i) – (ii) show that the presence of DMC will always preclude LEMC formation, the "survival" of LEMC in our SEI strongly suggests that the SEI formation *must* occur in a DMC-free region, and we attribute this to the presence of the ordered electrical double layer discussed above (Scheme 4). The SEI formation mechanism agrees well with our model chemical system described in (***iii***), the EDL models proposed in the literature,[68, 69] as well as the "dictation" of SEI formation by Li^+ solvation structure reported previously.[63, 64, 70, 71]

In our model, before a complete SEI coverage, we expect some degree of solvent penetration (Li^+-EC complex) into the outer layer of the MC/S composite, leading to a partial solvation of S^{2-} by EC. The subsequent fast chemical reactions of S^{2-} with surround Li^+-EC confined in the near-surface region of the MC/S cathode (see Scheme 4) generate SEI. The initial nucleophilic addition between the sulfide and the activated EC molecule gives rise to DLEMTC, which further reacts with a second activated EC molecule to give LEMC (Scheme 1, path A). This SEI formation consumes significant quantities of sulfur at the near-surface region of the cathode (*ca*. 40% of active sulfur), but once the SEI is established in the first few charge-discharge cycles, further sulfur reactions are completely shut down. This chemical stability is evidenced by near 100 % coulombic efficiency for thousands of cycles.[12] As such, the LEMC-based SEI completely blocks the corrosion process and prevents any shuttling of sulfides between cathode and anode. Such stability is only obtained through a combination of the LEMC based SEI *and* the use of the 5 Å microporous carbon to entrap the redox active sulfur species. While the microporous carbon does not contain rigorously monodisperse pore sizes, the pore size distributions are relatively monodispersed.[12] Multiple works have shown that this pore structure is critical to the cathode stability in that larger and less-uniform pore structures produce significantly less stable cathodes (e.g., "polysulfide shuttling").[2, 3, 10] With the 5 Å microporous carbon support, the status of entrapped sulfur (which we believe to be S_2 and not S_8) and lithiation/dethiation mechanism (the "quasi-solid-state" mechanism, see below) should be quite uniform throughout the MC/S cathode.

In addition to LEMC, LMC is also present as a minor component in the SEI structure. The formation of LMC results from a heterogeneous and sluggish reaction between $DMC_{(l)}$ and $LEMC_{(s)}$ that has been documented elsewhere.[36] Since LEMC has relatively high Li^+ conductivity (10^{-6} S/cm) but LMC is Li^+ insulating, Li^+ transport through the SEI is presumably facilitated by LEMC, while incorporation of LMC in the SEI may have detrimental influences.

These results also show that the Li^+ ions are completely desolvated after entering the SEI. If residual solvent molecules were transported through the SEI into the active MC/S electrode, sulfur would continually be consumed, coulombic efficiencies would be less than 100% and cycle life would be limited. The observed stabilities and high coulombic efficiencies show that these subsequent corrosion reactions are not occurring and only Li^+ ions enter/leave the active MC/S cathode. As such, sulfur lithiation in the microporous carbon host occurs through a solid-solid transition, which is consistent with the "quasi-solid-state" mechanism reported previously.[13] The mechanism features a single phase transition (solid-state neutral S^0 to solid-state S^{2-}) without any solvation of intermediates, and gives only one discharge/charge plateau. This feature is in contrast with the multi-plateau behavior observed in ethereal Li-S batteries.[1]

Sulfur is known to suffer from large volume changes upon battery charge/discharge. However, in the present case, volume change does not appear to significantly affect cathode performance since the sulfur is entrapped in carbon host, which serves as a "buffer" for the volume changes of $S + 2e^- \leftrightarrow S^{2-}$. The sulfur loading in the MC/S composite is relatively low (*ca.* 20% by mass) compared with other C-S composites, further alleviating the volume change issue. We reason that this "buffering functionality" may be critical for the superior cycling stability of the Li-S battery based on the SEI-covered MC/S composite. The long-term cycling stability of these cathodes provides evidence for this stability.[12]

Finally, we note that lithiation of sulfur in the micropore cavities of the carbon host can give Li_2S in the completely discharged state but the limited pore volume of the carbon micropores would preclude the formation of "bulk" Li_2S crystallites. While the stoichiometry of the fully lithiated state would be Li_2S in the microporous structure, the S^{2-} ions could not achieve the cubic coordination environment with eight nearest neighboring Li^+ (Li_8--S) present in the bulk Li_2S phase.[72] Such under-coordination of the S^{2-} ion (*i.e.* Li_{8-x}--S where x = *ca*. 2-4) results in diminished stabilization of the negative charge on the sulfide ion, which results in anomalously low 2p sulfur binding energies in the XPS spectra of the discharged MC/S cathodes.[12] Due to the sub-nano confinement, we expect the as-formed Li_2S is amorphous with aggregates of 2-3 Li_2S molecules held together by the ionic interactions between Li^+, S^{2-} and the surrounding carbon wall. As such, the S^{2-} ions have fewer than 6 Li^+ ions in their coordination sphere and cannot form the bulk Li_2S structure.

Scheme 4. Schematic representation of the EDL structure of a polarized MC/S cathode in a Li-MC/S battery during initial discharge and SEI formation.

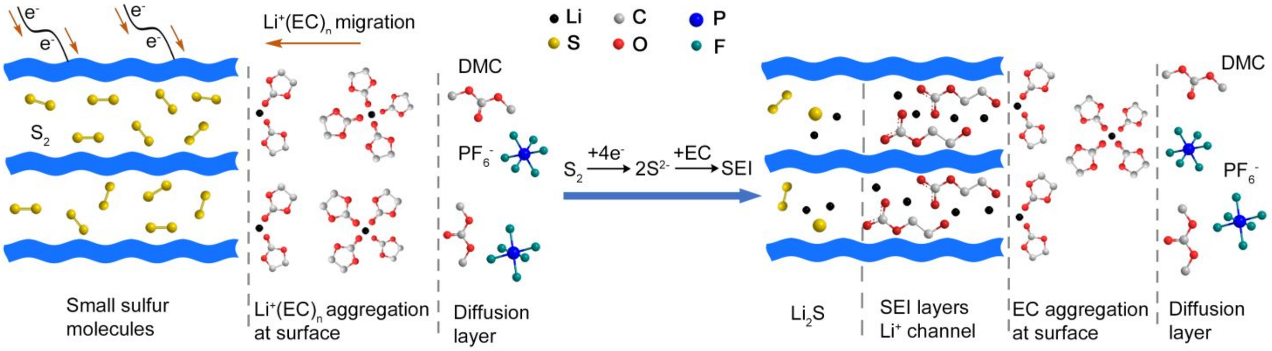

Conclusions

Through the combination of model chemical reactions, DFT simulations and direct analysis of authentic SEIs by NMR spectroscopy, we have shown that the primary organic components of the MC/S cathode SEI are LEMC and LMC formed through multi-step chemical reactions. The roles of Li^+ in directing the formation of these SEI components are identified. The presence of an ordered EDL structure in cathode-electrolyte interface consisting of preferential solvation of Li^+ by EC excludes DMC from participating SEI formation, while Li^+-EC interaction favors nucleophilic attack of sulfide at the carbonyl carbon of the coordinated EC molecules (Path A of Scheme 1). The major organic species of the SEIs on the sulfur cathode are virtually identical to those on graphitic anodes, but the SEIs on the two electrodes are generated through completely different mechanisms. The entrapment of the small sulfur molecules in the 5 Å micropores of the microporous carbon hosts *and* the coating of the LEMC/LMC SEI provides remarkable cycling stability through the complete elimination of corrosion reactions and sulfur shuttling once the SEI is formed. While SEI is likely to be formed with other sulfur cathodes employing EC/DMC electrolytes, cell stability seems to require both the LEMC SEI and the MC/S cathode with entrapped sulfur. These findings provide new fundamental insight into SEI formation on cathodes and suggest new avenues for artificial SEIs that preclude capacity loss.

ASSOCIATED CONTENT

The Supporting Information is available free of charge at:

Experimental and computational details; spectroscopic characterizations (1D and 2D NMR, FT-IR, ESI-MS and XRD) on the synthesized compounds; Electrochemical characterizations on the battery electrodes; Reaction schemes.

AUTHOR INFORMATION

Corresponding Authors

Bryan W. Eichhorn – *Department of Chemistry and Biochemistry, University of Maryland, College Park, MD, 20742, USA.*

Email: eichhorn@umd.edu

Kang Xu – *Electrochemistry Branch, Power and Energy Division Sensor and Electron Devices Directorate, U.S. Army Research Laboratory, Adelphi, MD, 20783, USA.*

Email: conrad.k.xu.civ@mail.mil

Chunsheng Wang – *Department of Chemical and Biomolecular Engineering, University of Maryland, College Park, MD, 20742, USA.*

Email: cswang@umd.edu

Authors

Luning Wang – *Department of Chemistry and Biochemistry, University of Maryland, College Park, MD, 20742, USA.*

Yuxiao Lin – *Department of Chemical Engineering and Materials Science, Michigan State University, East Lansing, Michigan 48824, USA.*

Samantha DeCarlo – *Department of Chemistry and Biochemistry, University of Maryland, College Park, MD, 20742, USA.*

Yi Wang – *Department of Chemistry and Biochemistry, University of Maryland, College Park, MD, 20742, USA.*

Kevin Leung – *Sandia National Laboratory, Albuquerque, NM 87185, USA.*

Yue Qi – *Department of Chemical Engineering and Materials Science, Michigan State University, East Lansing, Michigan 48824, USA.*

Complete contact information is available at:

Author Contributions

The manuscript was written through contributions of all authors. All authors have given approval to the final version of the manuscript.

Notes

The authors declare no competing financial interest.

ACKNOWLEDGEMENTS

We thank the DOE for funding this research through the EFRC (NEES-II). We thank Prof. Jeffery Davis for many helpful discussions. K.L. is was supported by Nanostructures for Electrical Energy Storage (NEES), an Energy Frontier Research Center funded by the U.S. Department of Energy, Office of Science, Office of Basic Energy Sciences under Award Number DESC0001160. Sandia National Laboratories is a multi-mission laboratory managed and operated by National Technology and Engineering Solutions of Sandia, LLC, a wholly owned subsidiary of Honeywell International, Inc., for the U.S. Department of Energy's National Nuclear Security Administration under contract DE-NA0003525. This paper describes objective technical results and analysis. Any subjective views or opinions that might be expressed in the paper do not necessarily represent the views of the U.S. Department of Energy or the United States Government.

REFERENCES

1. Ji, X.; Lee, K. T.; Nazar, L. F., A highly ordered nanostructured carbon–sulphur cathode for lithium–sulphur batteries. *Nature materials* **2009,** *8* (6), 500-506.

2. Manthiram, A.; Chung, S. H.; Zu, C., Lithium–Sulfur Batteries: Progress and Prospects. *Adv. Mater.* **2015,** *27* (12), 1980-2006.

3. Yin, Y. X.; Xin, S.; Guo, Y. G.; Wan, L. J., Lithium–sulfur batteries: Electrochemistry, materials, and prospects. *Angew. Chem. Int. Ed.* **2013,** *52* (50), 13186-13200.

4. Borchardt, L.; Oschatz, M.; Kaskel, S., Carbon Materials for Lithium Sulfur Batteries—Ten Critical Questions. *Chem. Eur. J.* **2016,** *22* (22), 7324-7351.

5. Barghamadi, M.; Kapoor, A.; Wen, C., A review on Li-S batteries as a high efficiency rechargeable lithium battery. *J. Electrochem. Soc.* **2013,** *160* (8), A1256-A1263.

6. Manthiram, A.; Fu, Y.; Chung, S.-H.; Zu, C.; Su, Y.-S., Rechargeable lithium–sulfur batteries. *Chem. Rev.* **2014,** *114* (23), 11751-11787.

7. Scheers, J.; Fantini, S.; Johansson, P., A review of electrolytes for lithium–sulphur batteries. *J. Power Sources* **2014,** *255*, 204-218.

8. Xu, K., Nonaqueous liquid electrolytes for lithium-based rechargeable batteries. *Chem. Rev.* **2004,** *104* (10), 4303-4418.

9. Whittingham, M. S., Lithium batteries and cathode materials. *Chem. Rev.* **2004,** *104* (10), 4271-4302.

10. Gao, J.; Lowe, M. A.; Kiya, Y.; Abruña, H. c. D., Effects of liquid electrolytes on the charge–discharge performance of rechargeable lithium/sulfur batteries: electrochemical and in-situ X-ray absorption spectroscopic studies. *J. Phys. Chem. C* **2011,** *115* (50), 25132-25137.

11. Yim, T.; Park, M.-S.; Yu, J.-S.; Kim, K. J.; Im, K. Y.; Kim, J.-H.; Jeong, G.; Jo, Y. N.; Woo, S.-G.; Kang, K. S., Effect of chemical reactivity of polysulfide toward carbonate-based electrolyte on the electrochemical performance of Li–S batteries. *Electrochim. Acta* **2013,** *107*, 454-460.

12. Xu, Y.; Wen, Y.; Zhu, Y.; Gaskell, K.; Cychosz, K. A.; Eichhorn, B.; Xu, K.; Wang, C., Confined Sulfur in Microporous Carbon Renders Superior Cycling Stability in Li/S Batteries. *Adv. Funct. Mater.* **2015,** *25* (27), 4312-4320.

13. Markevich, E.; Salitra, G.; Talyosef, Y.; Chesneau, F.; Aurbach, D., Review—On the Mechanism of Quasi-Solid-State Lithiation of Sulfur Encapsulated in Microporous Carbons: Is the Existence of Small Sulfur Molecules Necessary? *J. Electrochem. Soc.* **2017,** *164* (1), A6244-A6253.

14. Markevich, E.; Salitra, G.; Rosenman, A.; Talyosef, Y.; Chesneau, F.; Aurbach, D., The effect of a solid electrolyte interphase on the mechanism of operation of lithium–sulfur batteries. *J. Mater. Chem. A* **2015,** *3* (39), 19873-19883.

15. Markevich, E.; Salitra, G.; Rosenman, A.; Talyosef, Y.; Chesneau, F.; Aurbach, D., Fluoroethylene carbonate as an important component in organic carbonate electrolyte solutions for lithium sulfur batteries. *Electrochem. Commun.* **2015,** *60*, 42-46.

16. Seh, Z. W.; Sun, Y.; Zhang, Q.; Cui, Y., Designing high-energy lithium–sulfur batteries. *Chem. Soc. Rev.* **2016,** *45* (20), 5605-5634.

17. Li, Z.; Yin, L., Nitrogen-doped MOF-derived micropores carbon as immobilizer for small sulfur molecules as a cathode for lithium sulfur batteries with excellent electrochemical performance. *ACS Appl. Mater. Interfaces* **2015,** *7* (7), 4029-4038.

18. Zheng, S.; Han, P.; Han, Z.; Zhang, H.; Tang, Z.; Yang, J., High performance C/S composite cathodes with conventional carbonate-based electrolytes in Li-S battery. *Sci. Rep.* **2014,** *4*, 4842.

19. Xin, S.; Gu, L.; Zhao, N.-H.; Yin, Y.-X.; Zhou, L.-J.; Guo, Y.-G.; Wan, L.-J., Smaller Sulfur Molecules Promise Better Lithium–Sulfur Batteries. *Journal of the American Chemical Society* **2012,** *134* (45), 18510-18513.

20. Wang, D.-W.; Zhou, G.; Li, F.; Wu, K.-H.; Lu, G. Q. M.; Cheng, H.-M.; Gentle, I. R., A microporous–mesoporous carbon with graphitic structure for a high-rate stable sulfur cathode in carbonate solvent-based Li–S batteries. *Phys. Chem. Chem. Phys.* **2012,** *14* (24), 8703-8710.

21. Zhang, B.; Qin, X.; Li, G.; Gao, X., Enhancement of long stability of sulfur cathode by encapsulating sulfur into micropores of carbon spheres. *Energy Environ. Sci.* **2010,** *3* (10), 1531-1537.

22. Zhang, W.; Qiao, D.; Pan, J.; Cao, Y.; Yang, H.; Ai, X., A Li+-conductive microporous carbon–sulfur composite for Li-S batteries. *Electrochim. Acta* **2013,** *87*, 497-502.

23. Li, X.; Lushington, A.; Sun, Q.; Xiao, W.; Liu, J.; Wang, B.; Ye, Y.; Nie, K.; Hu, Y.; Xiao, Q., Safe and durable high-temperature lithium–sulfur batteries via molecular layer deposited coating. *Nano Lett.* **2016,** *16* (6), 3545-3549.

24. Lee, J. T.; Eom, K.; Wu, F.; Kim, H.; Lee, D. C.; Zdyrko, B.; Yushin, G., Enhancing the Stability of Sulfur Cathodes in Li–S Cells via in Situ Formation of a Solid Electrolyte Layer. *ACS Energy Lett.* **2016,** *1* (2), 373-379.

25. Li, X.; Liang, J.; Zhang, K.; Hou, Z.; Zhang, W.; Zhu, Y.; Qian, Y., Amorphous S-rich S 1− x Se x/C (x≤ 0.1) composites promise better lithium–sulfur batteries in a carbonate-based electrolyte. *Energy Environ. Sci.* **2015,** *8* (11), 3181-3186.

26. Fu, C.; Wong, B. M.; Bozhilov, K. N.; Guo, J., Solid state lithiation–delithiation of sulphur in sub-nano confinement: a new concept for designing lithium–sulphur batteries. *Chem. Sci.* **2016,** *7* (2), 1224-1232.

27. Li, Z.; Yuan, L.; Yi, Z.; Sun, Y.; Liu, Y.; Jiang, Y.; Shen, Y.; Xin, Y.; Zhang, Z.; Huang, Y., Insight into the Electrode Mechanism in Lithium-Sulfur Batteries with Ordered Microporous Carbon Confined Sulfur as the Cathode. *Adv. Energy Mater.* **2014,** *4* (7), 1301473.

28. Zheng, S.; Chen, Y.; Xu, Y.; Yi, F.; Zhu, Y.; Liu, Y.; Yang, J.; Wang, C., In situ formed lithium sulfide/microporous carbon cathodes for lithium-ion batteries. *ACS Nano* **2013,** *7* (12), 10995-11003.

29. Fanous, J.; Wegner, M.; Grimminger, J.; Andresen, A. n.; Buchmeiser, M. R., Structure-related electrochemistry of sulfur-poly (acrylonitrile) composite cathode materials for rechargeable lithium batteries. *Chem. Mater.* **2011,** *23* (22), 5024-5028.

30. Xu, G. L.; Sun, H.; Luo, C.; Estevez, L.; Zhuang, M.; Gao, H.; Amine, R.; Wang, H.; Zhang, X.; Sun, C. J., Solid-State Lithium/Selenium–Sulfur Chemistry Enabled via a Robust Solid-Electrolyte Interphase. *Adv. Energy Mater.* **2019,** *9* (2), 1802235.

31. Helen, M.; Reddy, M. A.; Diemant, T.; Golla-Schindler, U.; Behm, R. J.; Kaiser, U.; Fichtner, M., Single step transformation of sulphur to Li2S2/Li2S in Li-S batteries. *Sci. Rep.* **2015,** *5*, 12146.

32. Peled, E., The electrochemical behavior of alkali and alkaline earth metals in nonaqueous battery systems—the solid electrolyte interphase model. *J. Electrochem. Soc.* **1979,** *126* (12), 2047-2051.

33. Peled, E.; Menkin, S., SEI: past, present and future. *J. Electrochem. Soc.* **2017,** *164* (7), A1703-A1719.

34. Xu, K., Electrolytes and interphases in Li-ion batteries and beyond. *Chem. Rev.* **2014,** *114* (23), 11503-11618.

35. Winter, M.; Barnett, B.; Xu, K., Before Li ion batteries. *Chem. Rev.* **2018,** *118* (23), 11433-11456.

36. Wang, L.; Menakath, A.; Han, F.; Wang, Y.; Zavalij, P. Y.; Gaskell, K. J.; Borodin, O.; Iuga, D.; Brown, S. P.; Wang, C., Identifying the components of the solid–electrolyte interphase in Li-ion batteries. *Nat. Chem.* **2019,** *11* (9), 789-796.

37. Rosenman, A.; Markevich, E.; Salitra, G.; Talyosef, Y.; Chesneau, F.; Aurbach, D., Facile Synthesis and Very Stable Cycling of Polyvinylidene Dichloride Derived Carbon: Sulfur Composite Cathode. *J. Electrochem. Soc.* **2016,** *163* (9), A1829-A1835.

38. Gachot, G.; Grugeon, S.; Armand, M.; Pilard, S.; Guenot, P.; Tarascon, J.-M.; Laruelle, S., Deciphering the multi-step degradation mechanisms of carbonate-based electrolyte in Li batteries. *J. Power Sources* **2008,** *178* (1), 409-421.

39. Persson, K.; Hinuma, Y.; Meng, Y. S.; Van der Ven, A.; Ceder, G., Thermodynamic and kinetic properties of the Li-graphite system from first-principles calculations. *Phys. Rev. B* **2010,** *82* (12), 125416.

40. Delley, B., An all-electron numerical method for solving the local density functional for polyatomic molecules. *J. Chem. Phys.* **1990,** *92* (1), 508-517.

41. Verma, P.; Maire, P.; Novák, P., A review of the features and analyses of the solid electrolyte interphase in Li-ion batteries. *Electrochim. Acta* **2010,** *55* (22), 6332-6341.

42. Leifer, N.; Smart, M.; Prakash, G.; Gonzalez, L.; Sanchez, L.; Smith, K.; Bhalla, P.; Grey, C.; Greenbaum, S., 13C solid state NMR suggests unusual breakdown products in SEI formation on lithium ion electrodes. *J. Electrochem. Soc.* **2011,** *158* (5), A471-A480.

43. Michan, A. L.; Parimalam, B. S.; Leskes, M.; Kerber, R. N.; Yoon, T.; Grey, C. P.; Lucht, B. L., Fluoroethylene carbonate and vinylene carbonate reduction: understanding lithium-ion battery electrolyte additives and solid electrolyte interphase formation. *Chem. Mater.* **2016,** *28* (22), 8149-8159.

44. Aurbach, D.; Daroux, M.; Faguy, P.; Yeager, E., Identification of surface films formed on lithium in propylene carbonate solutions. *J. Electrochem. Soc.* **1987,** *134* (7), 1611-1620.

45. Goren, E.; Chusid, O.; Aurbach, D., The application of in situ FTIR spectroscopy to the study of surface films formed on lithium and noble metals at low potentials in Li battery electrolytes. *J. Electrochem. Soc.* **1991,** *138* (5), L6-L9.

46. Aurbach, D.; Markovsky, B.; Shechter, A.; Ein-Eli, Y.; Cohen, H., A comparative study of synthetic graphite and Li electrodes in electrolyte solutions based on ethylene carbonate-dimethyl carbonate mixtures. *J. Electrochem. Soc.* **1996,** *143* (12), 3809-3820.

47. Zhuang, G. V.; Ross, P. N., Analysis of the chemical composition of the passive film on Li-Ion battery anodes using attentuated total reflection infrared spectroscopy. *Electrochemical and solid-state letters* **2003,** *6* (7), A136-A139.

48. Zhuang, G.; Xu, K.; Jow, T.; Ross, P., Study of SEI layer formed on graphite anodes in PC/LiBOB electrolyte using IR spectroscopy. *Electrochemical and solid-state letters* **2004,** *7* (8), A224-A227.

49. Ross, P., Studies of Interfacial Chemistry in Lithium and Li-ion Battery Systems Using Infrared Spectroscopy. *ECS Trans.* **2006,** *1* (26), 161-170.

50. Kang, S.-H.; Abraham, D.; Xiao, A.; Lucht, B., Investigating the solid electrolyte interphase using binder-free graphite electrodes. *J. Power Sources* **2008,** *175* (1), 526-532.

51. Xiao, A.; Yang, L.; Lucht, B. L.; Kang, S.-H.; Abraham, D. P., Examining the solid electrolyte interphase on binder-free graphite electrodes. *J. Electrochem. Soc.* **2009,** *156* (4), A318-A327.

52. Nie, M.; Chalasani, D.; Abraham, D. P.; Chen, Y.; Bose, A.; Lucht, B. L., Lithium ion battery graphite solid electrolyte interphase revealed by microscopy and spectroscopy. *J. Phys. Chem. C* **2013,** *117* (3), 1257-1267.

53. Shkrob, I. A.; Zhu, Y.; Marin, T. W.; Abraham, D., Reduction of carbonate electrolytes and the formation of solid-electrolyte interface (SEI) in Lithium-Ion Batteries. 2. Radiolytically induced polymerization of ethylene carbonate. *J. Phys. Chem. C* **2013,** *117* (38), 19270-19279.

54. Michan, A. L.; Leskes, M.; Grey, C. P., Voltage dependent solid electrolyte interphase formation in silicon electrodes: Monitoring the formation of organic decomposition products. *Chem. Mater.* **2015,** *28* (1), 385-398.

55. Zhang, X.; Kostecki, R.; Richardson, T. J.; Pugh, J. K.; Ross, P. N., Electrochemical and infrared studies of the reduction of organic carbonates. *J. Electrochem. Soc.* **2001,** *148* (12), A1341-A1345.

56. Goodenough, J. B.; Kim, Y., Challenges for Rechargeable Li Batteries. *Chem. Mater.* **2010,** *22* (3), 587-603.

57. Wang, Y.; Nakamura, S.; Ue, M.; Balbuena, P. B., Theoretical studies to understand surface chemistry on carbon anodes for lithium-ion batteries: reduction mechanisms of ethylene carbonate. *Journal of the American Chemical Society* **2001,** *123* (47), 11708-11718.

58. Zhuang, G. V.; Yang, H.; Blizanac, B.; Ross, P. N., A study of electrochemical reduction of ethylene and propylene carbonate electrolytes on graphite using ATR-FTIR spectroscopy. *Electrochemical and Solid-State Letters* **2005,** *8* (9), A441-A445.

59. Shi, F.; Ross, P. N.; Zhao, H.; Liu, G.; Somorjai, G. A.; Komvopoulos, K., A Catalytic Path for Electrolyte Reduction in Lithium-Ion Cells Revealed by in Situ Attenuated Total Reflection-Fourier Transform Infrared Spectroscopy. *Journal of the American Chemical Society* **2015,** *137* (9), 3181-3184.

60. Sasaki, T.; Abe, T.; Iriyama, Y.; Inaba, M.; Ogumi, Z., Formation mechanism of alkyl dicarbonates in Li-ion cells. *J. Power Sources* **2005,** *150*, 208-215.

61. Yang, L.; Xiao, A.; Lucht, B. L., Investigation of solvation in lithium ion battery electrolytes by NMR spectroscopy. *J. Mol. Liq.* **2010,** *154* (2), 131-133.

62. Bogle, X.; Vazquez, R.; Greenbaum, S.; Cresce, A. v. W.; Xu, K., Understanding Li+–Solvent Interaction in Nonaqueous Carbonate Electrolytes with 17O NMR. *J. Phys. Chem. Lett.* **2013,** *4* (10), 1664-1668.

63. von Cresce, A.; Xu, K., Preferential solvation of Li+ directs formation of interphase on graphitic anode. *Electrochemical and Solid-State Letters* **2011,** *14* (10), A154-A156.

64. Xu, K.; von Wald Cresce, A., Li+-solvation/desolvation dictates interphasial processes on graphitic anode in Li ion cells. *J. Mater. Res.* **2012,** *27* (18), 2327-2341.

65. Yanase, S.; Oi, T., Solvation of lithium ion in organic electrolyte solutions and its isotopie reduced partition function ratios studied by Ab initio molecular orbital method. *Journal of nuclear science and technology* **2002,** *39* (10), 1060-1064.

66. Blint, R. J., Binding of ether and carbonyl oxygens to lithium ion. *J. Electrochem. Soc.* **1995,** *142* (3), 696-702.

67. Cazzanelli, E.; Croce, F.; Appetecchi, G. B.; Benevelli, F.; Mustarelli, P., Li+ solvation in ethylene carbonate–propylene carbonate concentrated solutions: A comprehensive model. *J. Chem. Phys.* **1997,** *107* (15), 5740-5747.

68. Borodin, O.; Ren, X.; Vatamanu, J.; von Wald Cresce, A.; Knap, J.; Xu, K., Modeling insight into battery electrolyte electrochemical stability and interfacial structure. *Acc. Chem. Res.* **2017,** *50* (12), 2886-2894.

69. Wang, F.; Borodin, O.; Ding, M. S.; Gobet, M.; Vatamanu, J.; Fan, X.; Gao, T.; Eidson, N.; Liang, Y.; Sun, W., Hybrid aqueous/non-aqueous electrolyte for safe and high-energy Li-ion batteries. *Joule* **2018,** *2* (5), 927-937.

70. von Wald Cresce, A.; Borodin, O.; Xu, K., Correlating Li+ solvation sheath structure with interphasial chemistry on graphite. *J. Phys. Chem. C* **2012,** *116* (50), 26111-26117.

71. Xu, K.; Lam, Y.; Zhang, S. S.; Jow, T. R.; Curtis, T. B., Solvation sheath of Li+ in nonaqueous electrolytes and its implication of graphite/electrolyte interface chemistry. *J. Phys. Chem. C* **2007,** *111* (20), 7411-7421.

72. Kubel, F.; Bertheville, B.; Bill, H., Crystal structure of dilithiumsulfide, Li2S. *Zeitschrift für Kristallographie-New Crystal Structures* **1999,** *214* (3), 302-302.

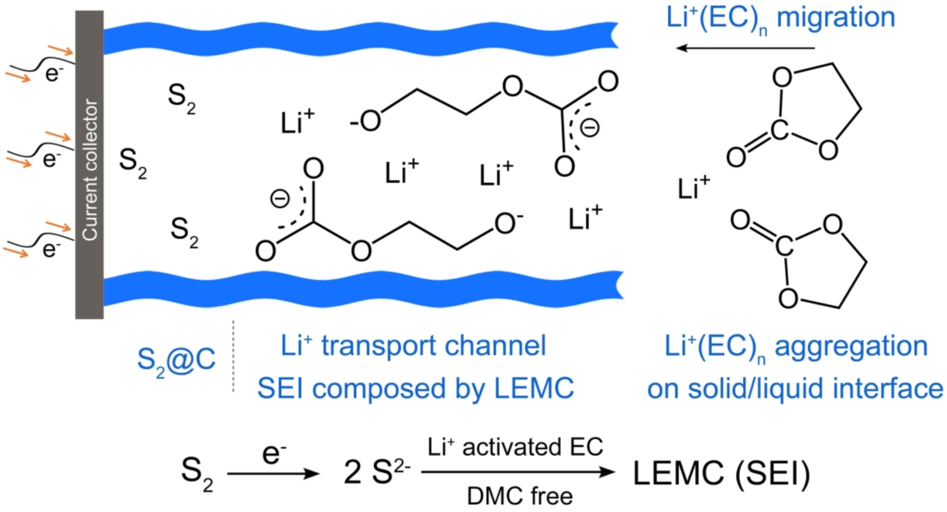

For Table of Contents Only

84x47mm (600 x 600 DPI)